# NAVAL RESEARCH LABORATORY

# SPACE SCIENCE DIVISION

# SOLAR AND HELIOSPHERIC PHYSICS BRANCH

Data Product Description Document and FITS Header Specification for the
Solar Orbiter Heliospheric Imager (SoloHI)

**SSD-SPC-SOLOHI-011 Rev. A** **24 January 2022**

**Approvals**

| | |
|---|---|
| Nathan Rich (Electronically Approved) | January 24, 2022 |
| SoloHI Ground Systems Lead | Date |
| Phil Hess (Electronically Approved) | January 24, 2022 |
| SoloHI Data Scientist | Date |
| Robin Colaninno (Electronically Approved) | January 24, 2022 |
| SoloHI Principal Investigator | Date |



**4555 Overlook Avenue, S.W.**
**Washington, D.C. 20375-5000**

**RECORD OF CHANGES**

| Revision Number | Date | Title or Brief Description | Entered By |
|---|---|---|---|
| - | 2021 Nov. 22 | Released Via ERN# SOLOHI-206. | D. Brooks |
| A | 2022 January 24 | Revised Per CCN# SSD-SPC-SOLOHI-011-001. | D. Brooks |
| | | | |
| | | | |
| | | | |
| | | | |
| | | | |

**TABLE OF CONTENTS**

1 INTRODUCTION ..... 1
1.1 Purpose ..... 1
1.2 Applicable Documents ..... 1
1.3 Reference Documents ..... 1
1.4 Acronyms and Abbreviations ..... 2
2 Overview ..... 4
2.1 SoloHI Instrument Description ..... 4
2.2 Science Objectives ..... 5
2.3 Data Generation Process ..... 5
2.4 Baseline Science Observing Program in Detail ..... 7
3 Scientific Measurements ..... 9
3.1 Coordinate System ..... 11
4 DATA PRODUCT DESCRIPTIONS ..... 12
4.1 Level-1 FITS ..... 14
4.2 Level-2 FITS ..... 14
4.2.1 Level-2b FITS: First-Order Backgrounds ..... 14
4.3 Level-3 Data Products ..... 15
4.3.1 Level-3 FITS ..... 15
4.3.2 Instrumental Artifacts Model ..... 16
4.3.3 Level-3 PNG ..... 16
4.3.4 Level-3 MPEG ..... 16
4.3.5 Level-3 MVI ..... 16
4.4 Revision Management ..... 16
5 FITS Header Definition ..... 17
5.1 Table Description ..... 17

5.2 Implementation.......... 17

5.3 Keyword Definition Table .......... 18

## TABLE OF FIGURES

Figure 2-1: SoloHI Instrument....................................................................................................4
Figure 2-2: SoloHI Concept of Operations........................................................................................6
Figure 2-4: SoloHI Observing Regions ..............................................................................................7
Figure 2-3: SoloHI Detector Mosaic...................................................................................................9
Figure 2-5: SoloHI Individual Region Example (Perihelion Shock Program)...............................10

# 1 INTRODUCTION

## 1.1 Purpose

This Data Product Description Document (DPDD) describes the format and content of the Solar Orbiter Heliospheric Imager (SoloHI) data. It includes descriptions of the data products and associated metadata, including the data format, content, and generation pipeline. These products will be stored and distributed from the Solar Orbiter Science Archive (SOAR) of ESA's Solar Orbiter Science Operations Center (SSOC).

The specifications described in this DPDD apply to all SoloHI Science products submitted to the SSOC. A similar document will be provided by the SOC, describing the SoloHI LL02 data that were generated at SOC after processing the LL01 data.

## 1.2 Applicable Documents

[METADATA] SOL-SGS-TN-0009,Rev2.2 Metadata Definition for Solar Orbiter Science Data

## 1.3 Reference Documents

| | |
|---|---|
| [FITSchecksum] | Checksum Keyword Convention, http://fits.gsfc.nasa.gov/registry/checksum/checksum.pdf |
| [FITSDOC] | Definition of the Flexible Image Transport System, http://fits.gsfc.nasa.gov/standard30/fits_standard30aa.pdf |
| [FITSDICT] | FITS Standard keyword definitions, http://heasarc.gsfc.nasa.gov/docs/fcg/standard_dict.html |
| [SODMP] | LWS-SO-PLAN-0008,RevB Solar Orbiter Project (NASA) Data Management Plan |
| [SCEICD] | NCST-ICD-HI003 SoloHI Camera Electronics Command Telemetry and Data Handling ICD |
| [TEMPLATE] | SOL-SGS-OTH-0004 Solar Orbiter Data Product Description Document template |
| [SOAR] | SOL-SGS-PL-0009, Solar Orbiter Archive Plan |
| [SOM] | SSD-DOC-SOLOHI-009, SoloHI Science Operations Manual (20161012) |
| [IUM] | SSD-DOC-SOLOHI-013,Rev J SoloHI Instrument User Manual |
| [LLDPDD] | SSD-DOC-SOLOHI-059,Rev B SoloHI Low Latency Data Product Description Document |

## 1.4 Acronyms and Abbreviations

| | |
|---|---|
| APS | Active Pixel Sensor |
| AU | Astronomical Unit |
| B | Brightness |
| BOL | Beginning of Life |
| CC | Camera Card |
| CCD | Charge Coupled Device |
| CCSDS | Consultative Committee for Space Data Systems |
| CME | Coronal Mass Ejection |
| CRS | Cosmic Ray Scrub in camera electronics |
| DIB | Detector Interface Board |
| DN | Digital Number |
| DPT | Data Processing Tool |
| DRB | Detector Readout Board |
| EDDS | EGOS Data Dissemination System |
| EID-A | Experiment Interface Document, Part A |
| EID-B | Experiment Interface Document, Part B |
| EOL | End of Life |
| FITS | Flexible Image Transport System for Astronomy |
| FOV | Field of View |
| FWHM | Full Width, Half Maximum |
| GSE | Ground Support Equipment |
| IGTAS | Instrument Ground Test Archival System |
| IRD | Instrument Requirements Document |
| LASCO | Large Angle and Spectrometric Coronagraph |
| LED | Light-emitting Diode |
| LL | Low Latency Data |
| LL01 | Low Latency Level 1 |
| LL02 | Low Latency Level 2 |
| MET | Mission Elapsed Time |
| MTF | Modulation Transfer Function |
| NIEL | Non-ionizing Energy Loss |
| NRL | Naval Research Laboratory |
| OPST | Observation Planning and Scheduling Tool |
| PC | Processor Card |
| PEC | Power Electronics Card |

| | |
|---|---|
| POC | Payload Operations Center |
| PSP | Parker Solar Probe |
| REC | Relay Electronics Card |
| ROI | Region of Interest |
| $R_{sun}$ | Solar Radius |
| SCE | SoloHI Camera Electronics |
| S/C | Spacecraft Bus |
| SECCHI | Sun Earth Connection Coronal and Heliospheric Investigation |
| SIM | SoloHI Instrument Module |
| SITD | Spacecraft and Instrument Telemetry Display |
| SNR | Signal to Noise Ratio |
| SOHO | Solar and Heliospheric Observatory |
| SoloHI | Solar Orbiter Heliospheric Imager |
| SOAR | Solar Orbiter Archive |
| SOOP | Solar Orbiter Observing Program |
| SPS | SoloHI Power System |
| SRD | Science Requirements Document |
| SSMM | Sold State Mass Memory |
| STEREO | Solar Terrestrial Relations Observatory |
| TID | Total Ionizing Dose |
| TDS | Telescope Development System |
| UFOV | Unobstructed Field of View |
| USB | Universal Serial Bus |
| WISPR | Wide-field Imager on Solar Probe |

## 2 Overview

The Solar Orbiter Heliospheric Imager (SoloHI) instrument for the ESA/NASA Solar Orbiter mission will track density fluctuations in the inner heliosphere, by observing visible sunlight scattered by electrons in the solar wind. Fluctuations are associated with dynamic events such as coronal mass ejections, but also with the "quiescent" solar wind. SoloHI will provide the crucial link between the low corona observations from the Solar Orbiter instruments and the in-situ measurements on Solar Orbiter.

### 2.1 SoloHI Instrument Description

SoloHI is a visible-light telescope, based on the SECCHI/Heliospheric Imager (HI) on the STEREO mission. In SoloHI, a series of baffles reduce the scattered light from the solar disk and reflections from the spacecraft to levels below the scene brightness, typically by a factor of $10^{12}$. The fluctuations are imposed against a much brighter signal produced by light scattered by dust particles (the zodiacal light/F-corona). SoloHI is a single telescope with a 48° optical field of view (FOV) beginning at approx. 5° from the Sun center.

**Figure 2-1: SoloHI Instrument**

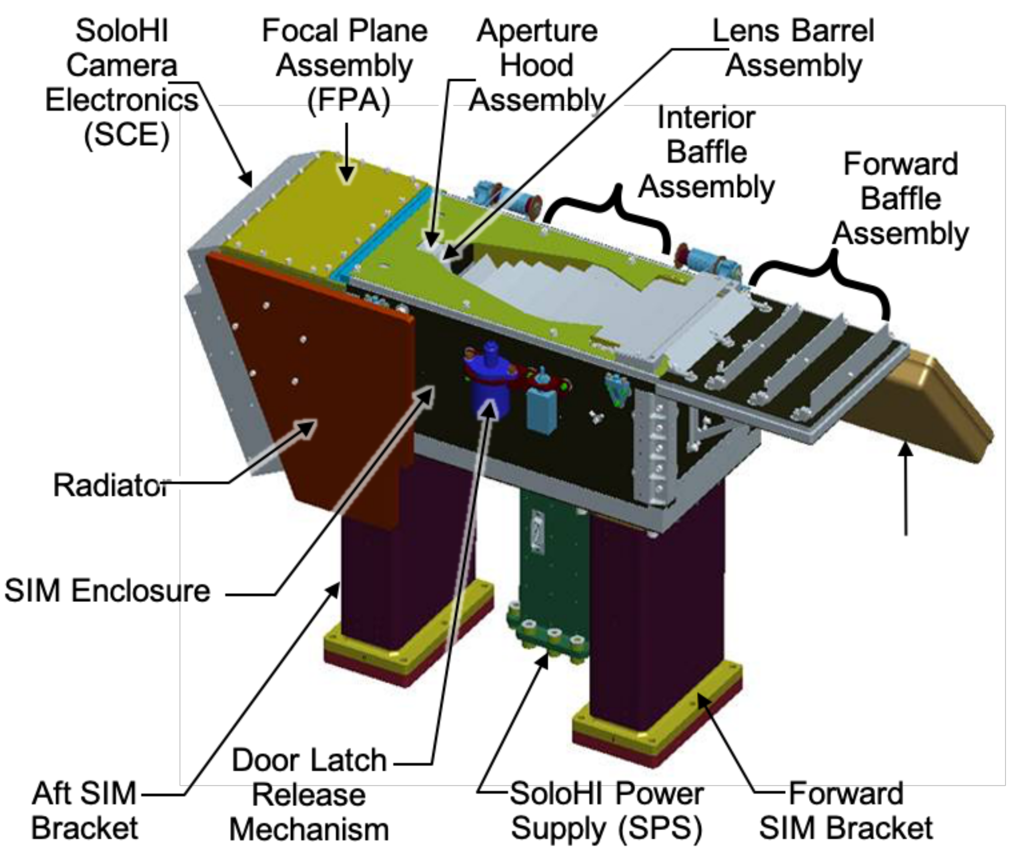

## 2.2 Science Objectives

SoloHI will be able to image the solar wind as it travels away from the Sun and impinges on Solar Orbiter and other inner heliospheric probes including Earth-orbiting instruments. SoloHI will have twice the field of view of the earlier SECCHI/HI1 instrument with improved spatial resolution, and comparable signal-to-noise ratio. As Solar Orbiter approaches the Sun, the instrument resolution will increase and the FOV will decrease relative to 1 AU. At perihelion, the SoloHI will have the same effective resolution as the SOHO LASCO/C2 coronagraph, with the same FOV size as LASCO/C3, but still with the same excellent signal-to-noise ratio. This vantage point will enable SoloHI to address the following Solar Obiter scientific questions:

- What are the origins of the solar wind streams and the heliospheric magnetic field?
- What are the sources, acceleration mechanisms, and transport processes of solar energetic particles?
- How do coronal mass ejections evolve in the inner heliosphere?
- What is the three-dimensional structure of the heliosphere?

SoloHI builds on the experience from the SECCHI instruments, on the NASA STEREO mission, and WISPR on PSP.

## 2.3 Data Generation Process

SoloHI image data packets are retrieved from the Solar Orbiter MOC via EDDS. They are then played back using the ITOS ground system to generate image files. The image files are then processed with an IDL procedure to decompress them and generate Level 1 FITS files. Further data products are generated using these files.

The SoloHI data products are produced by the SoloHI team at the SoloHI Science Processing and Data Center (SPDC) at NRL. A copy of the FITS data products resides at the Solar Data Archive Center (SDAC) at GSFC, and at the ESA SOAR in Spain. NRL will provide an online database query of the header keywords and the ability to download data that is pointed to be the query result.

**Figure 2-2: SoloHI Concept of Operations**

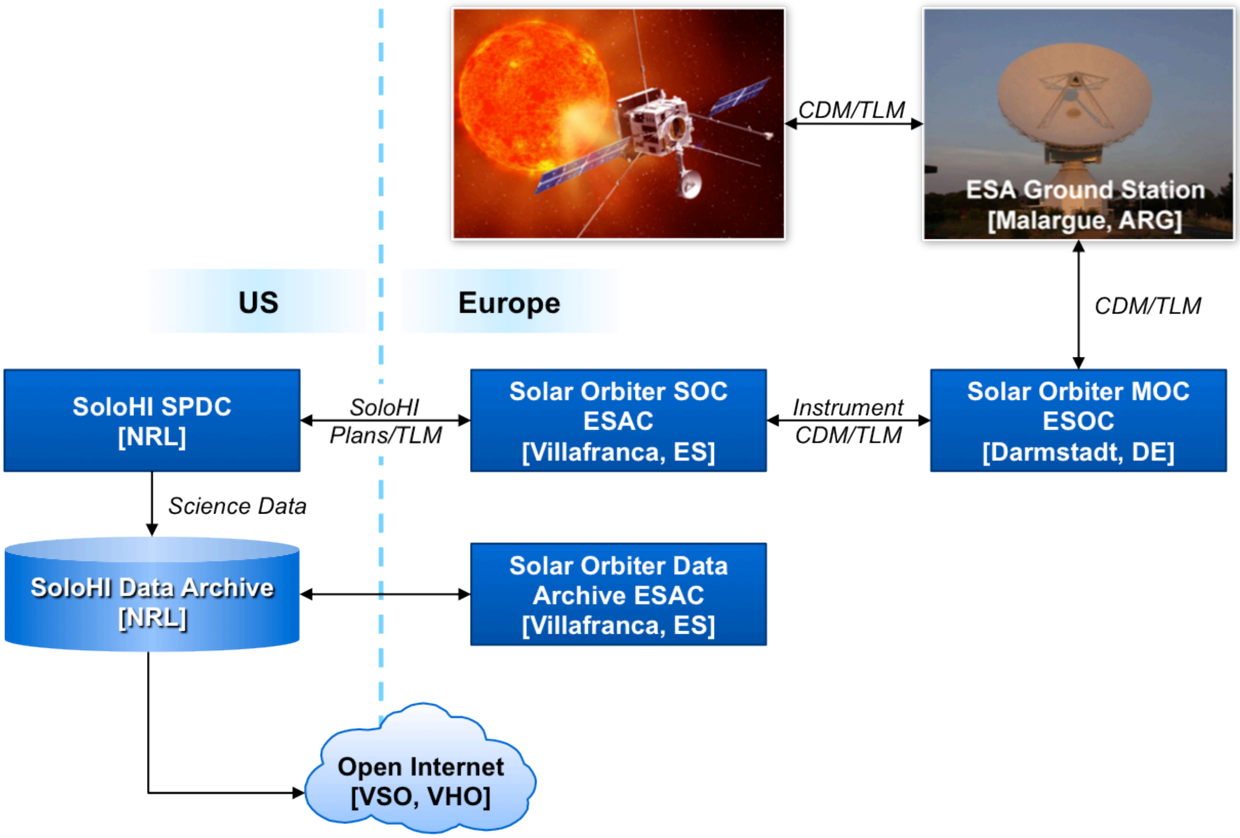


Figure 2-2 identifies the interfaces and concept of operations between the SoloHI Science Planning and Data Center (SPDC) at NRL and the Solar Orbiter Science Ground Segment (SGS). All receipt of telemetry from and commanding of the SoloHI instrument is via the Solar Orbiter Science Operations Center (SSOC) at the European Space Astronomy Center (ESA/ESAC) near Madrid. The Solar Orbiter Mission Operations Center (SMOC) and the spacecraft communications infrastructure are provided by the European Space Operations Center (ESA/ESOC) in Darmstadt.

The [IUM] SSD-DOC-SOLOHI-013 SoloHI Instrument User Manual was provided to the ESA/ESOC. The IMU includes details on housekeeping operation of the instrument and on-orbit contingency and safety procedures. The SoloHI team supports Solar Orbiter spacecraft and science operations meetings and functions as required. The SPDC specifies instrument commands to the SSOC to be coordinated with other instruments' commands for submission to the SMOC as consolidated payload operations requests. The SMOC in turn processes and merges the submitted requests into a timeline to be uplinked to the spacecraft. The SPDC receives and archives all instrument telemetry from the SSOC and provides data products to the science community as well as to the Solar Orbiter Data Archive at ESAC.

## 2.4 Baseline Science Observing Program in Detail

The SoloHI baseline observing program is be designed to satisfy the observing program requirements in the SoloHI Baseline science measurement requirements and to satisfy the SoloHI telemetry allocation. Nominally, SoloHI will be operated during three separate 10-day periods during each approximately 150-day orbit (30 days per orbit). Data will be stored on the onboard recorder SSMM for transmission to the ground during the contact period. A highly compressed subsets of the science data is provided as a quick-look preview in the low latency data pipeline describe in [LLDPDD] SSD-DOC-SOLOHI-059, SoloHI Low Latency Data Product Description Document.

**Figure 2-3: SoloHI Observing Regions**

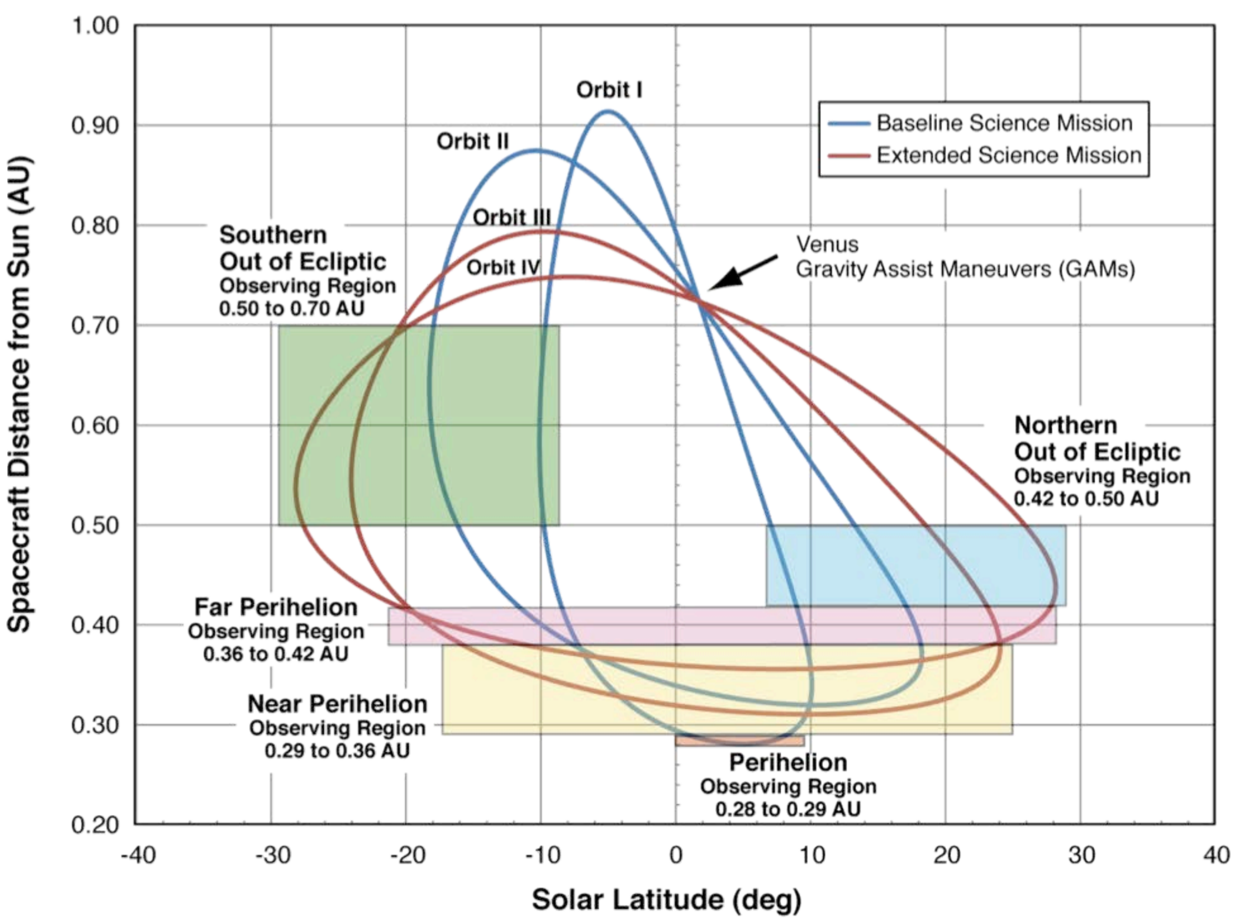


There are 8 orbits (LTP 05 – LTP 12) in the Baseline Science Nominal Mission Period (NMP) and an additional 8 orbits (LTP 13 – LTP 22) in the Extended Mission Period (EMP). If these 16 orbits are plotted as a function of the instrument distance from the sun and the solar latitude, as shown in Figure 2-4, it is apparent that there are only 4 unique orbits in the combined Solar Orbiter NMP and EMP. Specifically, there are 2 unique orbits for the Baseline science mission (Orbits I and II) and 2 unique orbits for the extended science mission (Orbits III and IV).

Nominally, the same set of synoptic observations will be taken during each orbit with similar characteristics. In addition to the synoptic observations, a number of critical periods have been identified during which we expect to increase the frequency and amount of SoloHI data above that contained in the baseline synoptic program.

Observations near perihelion will focus on science objectives that benefit from higher spatial or temporal resolution. Full resolution images will be obtained, and the FOV will be limited if necessary, by transmitting only a portion of each image to the onboard recorder.

The periods near maximum northern and southern heliolatitudes will be of particular interest for out-of-ecliptic observations of heliospheric structures. This will be particularly significant during the latter part of the NMP, and during the EMP, when the orbit inclination increases.

Special configurations of interest will occur at quadrature, and conjunction with Earth or other heliospheric probes such as STEREO, PSP or Bepi-Colombo. (Quadrature occurs when the probe lies on or near the Thomson surface.) Additional observations may be scheduled during these periods and during other periods of joint operations between multiple missions. The various types of observations may be coordinated with other Solar Orbiter instruments as part of a Solar Orbiter Observing Program (SOOP).

# 3 Scientific Measurements

SoloHI uses the new detector technology of Advanced Pixel Sensor (APS) developed by SRI. The SoloHI camera operates a mosaic of four 2048x1920 pixel detector tiles. The average plate scale is 35.5 arcsec/pixel. Each detector tile has 10 rows and 10 columns of opaque pixels, i.e. pixels shielded from light, which are used for measuring dark current and column-to-column variations. For each tile, multiple readouts are obtained over a period of several minutes and are summed on-board to create an image with increased the signal-to-noise ratio and to reduce the telemetry load.

Each corner of the mosaic has pixels that are not physically masked but also not fully illuminated by the optics. Figure 2-2 shows the position of the optical projection onto the detector mosaic, layout of each individual detector tile, and the masked rows and columns on the left and bottom edges. The size of the gap between detectors is 44 pixels.

Each detector tile is 2-side buttable, and is rotated 90° to keep the signal lines accessible to the perimeter. However, the 90° rotation also rotates the rows and columns and forces a different readout direction for each tile. The native origin of each image (lower left corner) as returned by the instrument is always the outer corner. As a result, re-assembly of the images into a full scene involves transposing as well as rotation.

**Figure 2-1: SoloHI Detector Mosaic**

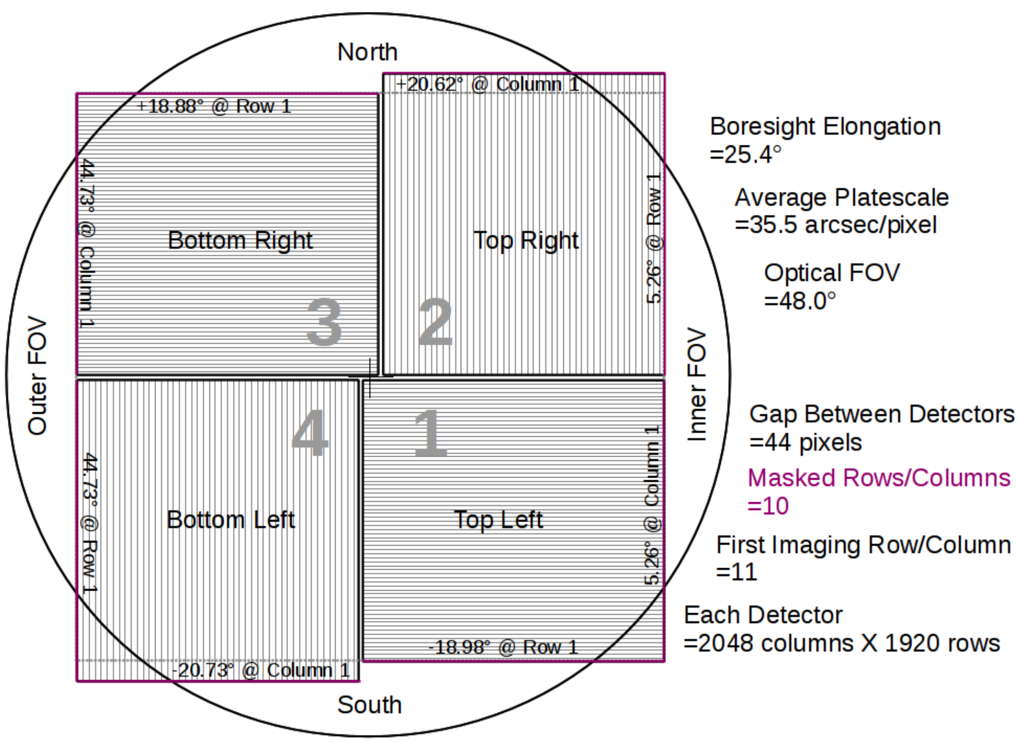


The camera electronics have 256 MB of memory and are capable of doing simple image processing. The three functions provided in the camera FPGA are cosmic ray scrub, pixel binning and image summing. Images are stored in the camera memory and then transferred to the LEON3FT processor for further image processing and image compression before being sent to the spacecraft. The LEON3FT manages the camera buffers in both the camera card and the processing card. The camera can read out regions of interest (ROI) on each detector depending upon the microcode and parameters loaded to its registers. Details of the onboard image process can be found in the [SOM] SSD-DOC-SOLOHI-009, SoloHI Science Operations Manual.

Scene readout is done by individual detector tiles, and more specifically by row. There are two readout chains so two readouts can be done at once, one using the outer detectors (top) and one using the inner (bottom) detectors. This also allows different settings for the outer and inner detectors. The readout is controlled by camera microcode that is uploaded to set the timing of each readout chain. The microcode reads register values to set parameters such as exposure time and image extent. Since the APS pixels are row and column addressed, they can be read out with different timing i.e. for a single detector tile one block of rows can be read out at a different rate than another, within the readout timing constraints of top or bottom and one row at a time.

To commence observing, the microcode is loaded to the camera along with settings of all of the registers. After being commanded to begin executing, individual exposures are sent to the camera electronics for initial processing. When a sum of exposures is finished, it is sent to the LEON3FT processor for further processing (such as compression) and packetization before being sent to the SSMM. The microcode runs in a continuous loop until commanded to stop.

**Figure 2-2: SoloHI Individual Region Example (Perihelion Shock Program)**

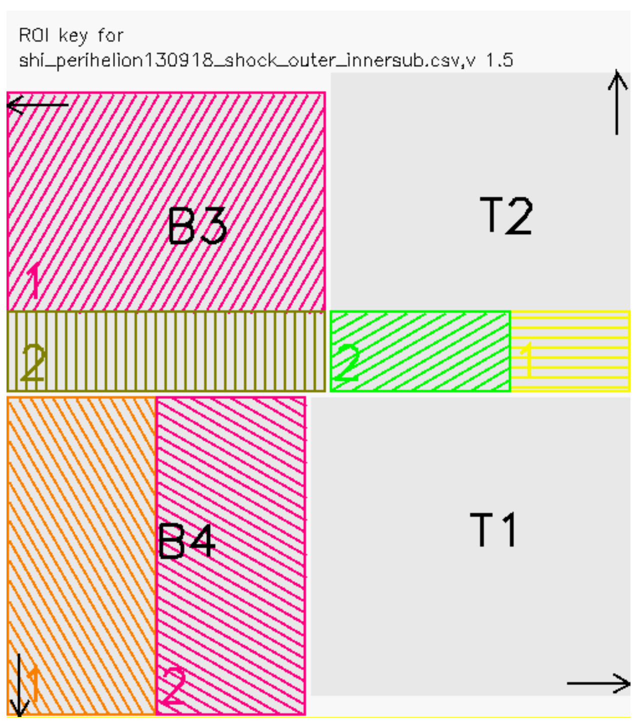

Figure 2-3 illustrates the various regions returned for a single observing program. A separate image file is generated for each region. The region numbers will correspond to the number of distinct regions in a given tile for each observing program, not specific ROIs defined by fixed pixel coordinates. For different observing sequences, the same region number in the same tile can correspond to different regions on the detector.

## 3.1 Coordinate System

SoloHI FITS files are annotated according the World Coordinate System [WCS]. Specifically, the SoloHI telescope relies on a zenith polynomial (ZPN) projection. These are described by nine keywords representing the distortion polynomial, PV1_j and PV2_j. The polynomial parameters in these keywords have been preliminarily derived from ground measurements and updated based on in-flight calibration data. In addition to the distortion, the other key parameters determined on the ground and since updated are the boresight pixel (CRPIXi) and the instrument roll matrix (PCi_j). The boresight pointing of the instrument (CRVALi) is determined from the SPICE kernel.

An image for a given tile from the mosaic is read out from the detector and must be rectified (rotated and/or transposed) to form the mosaic. The rectification is unique for each tile. Because the individual tiles form a single optical system, the distortion coefficients, roll matrix and boresight pointing are the same regardless of tile and rectification. The boresight pixel will be unique to each tile, based on its relative location within the mosaic.

Tile-Specific Rectification Operation:

| Tile | Rotation (counter-clockwise) | Transposed? |
|---|---|---|
| 1 | 90° | Yes |
| 2 | 180° | Yes |
| 3 | 270° | Yes |
| 4 | 0° | No |

# 4 DATA PRODUCT DESCRIPTIONS

The SoloHI filenames are defined by solo_L#_descriptor_YYYYMMDDHHMMSS_V#.fits where L# and V# refer to the processing level and version number of the file, respectively. The SoloHI data descriptor is defined as “solohi-XYZ”, with each “XYZ” character encoding different information about the file. The possible values of ‘X’, ‘Y’ and ‘Z’ are:

| X | | Y | | Z | |
|---|---|---|---|---|---|
| Value | Definition | Value | Definition | Value | Definition |
| 1 | Tile 1 | f | Full field without bias subtraction | b | Bias Image |
| 2 | Tile 2 | g | Full field with bias subtraction | h | Header Only |
| 3 | Tile 3 | u | Subfield without bias subtraction | s | Sum of multiple exposures, full resolution |
| 4 | Tile 4 | v | Subfield with bias subtraction | t | Sum of multiple exposures, binned |
| m | Mosaic of all tiles | | | f | Single exposure, full resolution |
| | | | | g | Single exposure, binned |

The SoloHI team distinguishes between “quick-look” and “released” data products. The quick-look products are generated as soon as they are received and may be reprocessed several times until the released product is produced. A “released” data product is produced on a per-orbit basis, about 3 months after the data for a full orbit has been received.

| Data Level | Product Title | Contents | Volume (GB/orbit) | Format | Latency | Frequency |
|---|---|---|---|---|---|---|
| L1 | Level-1 quick-look | uncalibrated image data | 23 | FITS | 7 days | as received; track-dependent |
| L1 | Level-1 released | uncalibrated image data | 23 | FITS | $T_0$+ 7 days | per orbit |
| L2 | Level-2 quick-look * | calibrated image data | 23 | FITS | $T_0$+ 7 days | as received; track-dependent |
| L2 | Level-2 released | calibrated L1 images | 23 | FITS | $T_0$+ 3 months | per orbit |

| | | | | | | |
|---|---|---|---|---|---|---|
| L2b | Level-2b released | calibrated backgrounds | 15 | FITS | $T_0$+ 1 orbit | per orbit |
| L3 | Background-subtracted quick-look | calibrated images with background removed | 23 | FITS | $T_0$+ 14 days | per orbit |
| L3 | Background-subtracted released | calibrated images with background removed | 23 | FITS | $T_0$+ 1 orbit | per orbit |
| L3 | Browse images (quick-look and released) | uncalibrated binned images with background removed, and compressed | 2 | PNG, JPG | varies with level | per orbit |
| L3 | Browse movies | browse images | 15 | MPG, MVI | varies with level | per orbit |
| L3 | Jmaps | time-elongation plots, uncalibrated | 1.5 | PNG | TBD | per orbit |
| L3 | syncronic or Carrington maps | heliospheric brightness at selected elongation angles | 0.15 | FITS, PNG | TBD | per orbit |
| L4 | CME masses | | 2 | FITS | $T_0$+ years | annually |

In the following table $T_0$ represents the time after the last data from a given orbit have been received at NRL.

**Table 1: Summary of SoloHI Data Products**

* The SoloHI L2 quick-look data is an interim product providing an initial look at the observations before complete processing and calibration. The L2 "Released" data set will supersede the quick-look L2. When the calibration is updated (infrequently), the SoloHI team will regenerate the Level-2 data. A best and final Level-2 dataset will be provided after end of mission (Phase F).

## 4.1 Level-1 FITS

The SoloHI Level-1 FITS data are de-compressed uncalibrated image data with no correction applied, except for rectification so that solar north is (approximately) up. Each detector tile is a separate file using the detector number from Figure 1 to specify tile. Data units are DN. Individual sub-fields are separate files.

Files are organized by date. In addition, there is a sub-category called “highcadence” for high cadence subfields.

## 4.2 Level-2 FITS

The Level-2 data are calibrated Level-1 files in units of Mean Solar Brightness (MSB). Every pixel is multiplied by a correction factor determined on the ground as a function of intensity in the pixel to account for the non-linearity of the detector, particularly at high intensities. If a bias image has not been subtracted onboard, a bias based on the masked pixels of the detector is subtracted. Any additional offset term applied for on-board bias subtraction to prevent negative values is determined from the remnant signal in the masked pixels and removed. If the image was binned to reduce size by combining pixels, the image is divided by the number of original pixels that make up each binned pixel. If the image has been truncated onboard (divided by $2^n$) the array is multiplied by the same. Next, the image is divided by the exposure time to convert the data from DN to DN/s. A vignetting correction function is applied to the image. Lastly, a calibration factor determined from stellar photometry is used to convert the data from DN/s to MSB.

Files are organized as in L1. There is a 1-1 relationship between L1 and L2 FITS files.

Software is provided to combine the individual Level 1 and Level 2 images into a detector mosaic.

### 4.2.1 Level-2b FITS: First-Order Backgrounds

An individual background model is created for each individual Level-2 single tile image. The first of three steps in the process is aimed at determining a pseudo-noise average level of each individual image as a function of image column, hereafter the $\sigma$-level of the image. (For computational purposes, each image is resized to 960x1024 regardless of the original size). In this way, the noise of each individual image is characterized by an array of 960 elements ($\sigma^i_j$; where *i* represents the image processed and *j* the column number). To minimize the detrimental effect of image to image variation resulting from the statistical nature of the algorithm (if uncorrected it would introduce a flickering in the time evolution of the overall background intensity), as many images as possible must be processed to allow for the large-scale homogenization of the pseudo-noise model.

The second step is a 2-stage statistical modeling of the individual column profile brightness of each image that exploits the smooth variation of the F corona and the known break in spatial scales between K-coronal features of interest and the broad contributions from F and stray light elements of the background (hereafter $B^i_j$).

Finally, the third step is the determination of the base brightness level of each individual model computed in step 2. This is done by subtracting 3 times $\sigma^i_j$ to each $B^i_j$. The resulting products (hereafter L2b) are the first-order background models for the corresponding individual L2 images.

## 4.3 Level-3 Data Products

Further processing (e.g., background subtracted images corrected by instrumental artifacts) and user-friendly sets for easy visualization are Level-3 (they may or may not have calibrated units). The latter includes, e.g. browse images, movies (of browse images), height-time maps/plots (Jmaps), Carrington maps, etc. Format may be FITS, PNG, MPEG, etc. as appropriate.

### 4.3.1 Level-3 FITS

This section provides a general outline of the Level-3 FITS processing. The procedure is in continuous development as we increase our understanding of the factors involved.

The purpose of the L3 data products is to reveal the dynamics of the faint K-corona signal. This is achieved by removing the background brightness from the L2 data (i.e., calibrated data in mean solar brightness units --MSB). Here we are defining background signal as everything but the K-corona. Because of the orbital characteristic of the Solar Orbiter mission (eccentric orbits with large changes in latitude), the background removal is a complex process. Briefly, this process involves the construction of a first-order background for each individual SoloHI image (L2b images) and the subsequent computation of a "grand minimum model" to account for the instrumental artifacts.

Once the individual first-order background models are computed, the corresponding background difference images are created. These difference images clearly show the faint K-corona signal. However, since the L2b background models do not include any artifact of an instrumental nature, the procedure enhances the relative contribution of this unwanted signal. But, the F-corona signal in the difference images is now absent, the creation of an instrumental artifacts model is possible by exploiting the time-domain.

These difference images corrected by the instrumental artifacts model will constitute the SoloHI Level-3 FITS data product. The files are organized by orbit, detector, and then date.

The process to generate the L3 FITS data product requires regular cadence of a given type of observation over a long period. As a result, some observations appearing in L1 and L2 may not have a L3 product. These include intermittent partial-frame subfields and high cadence data.

Full FOV mosaic images are provided as a Level-3 data product. There is a 4-1 relationship between L1 and L2 FITS files.

### 4.3.2 Instrumental Artifacts Model

To create the instrumental artifact model (one per interval per tile per bin size set), we follow the well-known and already established technique of computing the models as the 10-percentile signal over the time period. (We use a 10-percentile rather than the minimum to exclude the effect of outliers.)

A well-known problem of this approach is the remnant signal in the model that could arise from pseudo-stationary K-corona features (e.g., a long-lived streamer) in the time period considered. Near co-rotation of the S/C with the Sun (about $\pm 7^{\circ}$) during the time period of the observations make this problematic. To date, we have not found a way to fully circumvent this issue. However, we did implement a procedure to mitigate the artifacts introduced by the presence of a remnant coronal signal in this model.

The use of the 10-percentile can introduce a difference between orbits, due to the varying distance from the Sun. The brightness distribution falls off with heliocentric distance, so images that are furthest from the Sun will contribute the most to the 10-percentile. If the observations don't all have the same range of heliocentric distances, then the 10-percentile level will be different between windows.

### 4.3.3 Level-3 PNG

These are browse images to allow quick viewing of the contents of the FITS files. There is a 1-1 correspondence between a file in the rel/fits/ directory and PNG files. File names (and path) match the FITS filenames except for the suffix. The images are byte-scaled to best illustrate the content of the image. Each level of FITS is scaled somewhat differently:

- L3: Data is scaled so the median is around 1.0 and corrected for sun distance.

### 4.3.4 Level-3 MPEG

MPEG format animations from the L3 FITS combine the 4 tiles and maps them onto an ARC projection. They are scaled in a manner similar to the L3 PNGs.

### 4.3.5 Level-3 MVI

The MVI format was internally developed at NRL as a simple method for storing image data along with metadata for each frame. They are not compressed.

## 4.4 Revision Management

The data product version number indicates how many times the product has been regenerated. Modifications to processing software, changes to calibration or other input files, and header (metadata) changes are all examples that would cause the version number to increase. Data entry errors, transmission problems or other types of failures may also cause a product to be re-released and thus have the data product version number incremented. The data product version is tracked by the VERSION keyword in the FITS header and also indicated in the filename. Version zero (V0) in the filename indicates a quicklook data product; it's VERSION number in the header may increment but the quicklook filename will not change.

# 5 FITS Header Definition

## 5.1 Table Description

The following table has 6 columns: KEYWORD, TYPE, VALUES/UNIT, DESCRIPTION, and SOURCE:

KEYWORD gives the name of the FITS keyword and may be up to 8 characters.

TYPE refers to the data type of the header value:

| | |
|---|---|
| S | String (max 68 chars) |
| I | Integer |
| R | Real |
| L | Logical (ASCII char, T or F) |

The size of the data depends upon the data type. For example, S2 is a 2-character string, whereas I2 is a 2 byte integer (16 bits).

VALUES: shows the range of values that the KEYWORD can take. If they values is a physical quantity then the unit are given.

DESCRIPTION: gives a short description of the keyword.

SOURCE: gives information about where the keyword value comes from.

- "BSF" implies the value is read directly from the command and put in the image header
- "FSW" implies the value is computed by FSW or read from a camera register

## 5.2 Implementation

This document is implemented in the SolarSoft procedures define_solohi_hdr.pro,v 1.62 and make_solohi_hdr.pro.

## 5.3 Keyword Definition Table

| KEYWORD | TYPE | VALUES | DESCRIPTION | SOURCE |
|---|---|---|---|---|
| APID | I*2 | Any | Integer Application ID for the telemetry from which this image is generated. | FSW shdr.FILE_RAW |
| BITPIX | I*2 | 16, 32, -32, -64 | Number of bits per pixel (multiple of 8) | FITS |
| BLANK | I*16 | -32768, 0 | -32768 for UINT, 0 for LONG, otherwise ignored | Pipeline |
| BSCALE | R*4 | Any | For FITS use only. If missing, then assumed to be 1: output data = FITS data * BSCALE + BZERO | Constant |
| BUNIT | S*20 | DN DN/s UNITLES S MSB etc. | Physical unit of array values (after BZERO and BSCALE, if present, are applied) | Definition |
| BZERO | R*4 | Any | For FITS use only. Physical value for the array value 0. If missing, then assumed to be zero. | Pipeline |
| CAMERA | S*5 | FM | Version of SoloHI Camera Electronics | Constant |
| CAR_ROT | I*2 | Num | Carrington Rotation number | Sunspice |
| CC2_i | I*2 | Any | Group 2 Bias | FSW basehdr.CC2_i |
| CC6_i | I*2 | Any | Group 6 Bias | FSW basehdr.CC6_i |
| CCBOTUCO | I*2 | Any | Version ID of Readout ucode used on Bottom | FSW basehdr.CCbotUcode |
| CCEXPCTL | I*2 | Any | CC Parameters | FSW basehdr.CCexpctrl |
| CCIMGCNT | I*2 | Any | Counter of images sent from camera to SDRAM | FSW basehdr.CCImgCntr |
| CCISUCOD | I*2 | Any | Version ID of Sequencer ucode used | FSW basehdr.CCisUcode |

| KEYWORD | TYPE | VALUES | DESCRIPTION | SOURCE |
|---|---|---|---|---|
| CCREPEAT | I*2 | Any | Num of images for CC task to take of this type | FSW basehdr.numPerROI |
| CCSEQTIM | I*2 | Any | Current value of sequence timer in microcode. | FSW basehdr.CCSeqTime |
| CCTOPUCO | I*2 | Any | Version ID of ucode used on Top | FSW basehdr.CCtopUcode |
| CCUCODE | S*3 | Any | Subscript of Readout Microcode from ucdtbldt.img or isreadout.cpp for this image (5 LSB of ccTopUcode or ccBotUcode) | FSW basehdr.CCtopUcode or basehdr.CCbotUcode |
| CDELT1 | R*4 | Deg | Coordinate increment at reference point (platescale) for horizontal axis | Calibration |
| CDELT1A | R*4 | Deg | Coordinate increment at reference point (platescale) for horizontal axis | Calibration |
| CDELT2 | R*4 | Deg | Coordinate increment at reference point (platescale) for vertical axis | Calibration |
| CDELT2A | R*4 | Deg | Coordinate increment at reference point (platescale) for vertical axis | Calibration |
| CHECKSUM | S | | String whose value forces the 32-bit 1's complement checksum accumulated over the entire FITS HDU to equal negative 0 | Pipeline |
| COMMENT | S*71 | Any | Comment. Can be repeated. | Varies |
| COMP_RAT | R*4 | ≥ 1.0 | Uncompressed/compressed quality ratio. Nominally, the compressed information content divided by the uncompressed information content, expressed as a percentage. The aim of a numeric value is to have a sortable item, so that users/programs can pick the best observation that satisfies any other (search) criteria. | Pipeline, XFBYTES |

| KEYWORD | TYPE | VALUES | DESCRIPTION | SOURCE |
|---|---|---|---|---|
| COMPRESS | S*19 | Type of compression | Lossless' - Data compression quality choice among 5 possible words, see description String A cross-instrument description of the data compression quality None - no compression applied Lossless - lossless compression, Lossy-high quality - lossy compression applied. Data quality is mostly unaffected. Lossy-strong - strong lossy compression applied. Analysis of data should take into account frequent compression artefacts. Lossy-extreme - extreme lossy compression applied. Data quality is visibly affected | Derived from basehdr.ipcmdlog |
| COSMICR | L | F(T) | Cosmic Ray Removal was enabled. | FSW basehdr.cccrs |
| COSMICS | I*4 | Any | Number of pixels changed by Cosimic Ray Removal | FSW basehdr.CRSreport |
| CREATOR | S*3 | --> | <software name + version> / FITS creation software & version | Pipeline |
| CRLN_OBS | R*8 | Deg | S/C Carrington longitude | Sunspice |
| CRLT_OBS | R*8 | Deg | S/C Carrington latitude | Sunspice |
| CRPIX1 | R*4 | Any | Pixel coordinate of reference point on horizontal axis | Calibration |
| CRPIX1A | R*4 | Any | Pixel coordinate of reference point on horizontal axis | Calibration |
| CRPIX2 | R*4 | Any | Pixel coordinate of reference point on vertical axis | Calibration |
| CRPIX2A | R*4 | Any | Pixel coordinate of reference point on vertical axis | Calibration |
| CRVAL1 | R*4 | Deg | Coordinate of reference point, reference frame horizontal axis | SPICE |

| KEYWORD | TYPE | VALUES | DESCRIPTION | SOURCE |
|---|---|---|---|---|
| CRVAL1A | R*4 | Deg | Coordinate of reference point, reference frame horizontal axis | SPICE |
| CRVAL2 | R*4 | Deg | Coordinate of reference point, reference frame vertical axis | SPICE |
| CRVAL2A | R*4 | Deg | Coordinate of reference point, reference frame vertical axis | SPICE |
| CTYPE1 | S*8 | HPLN-ZPN | WCS axis X | Constant |
| CTYPE1A | S*8 | RA---ZPN | WCS axis X P | Constant |
| CTYPE2 | S*8 | HPLT-ZPN | WCS axis Y | Constant |
| CTYPE2A | S*8 | DEC--ZPN | WCS axis Y P | Constant |
| CUNIT1 | S*3 | Deg | Units of coordinate increment and value | Constant |
| CUNIT1A | S*3 | Deg | Units of coordinate increment and value | Constant |
| CUNIT2 | S*3 | Deg | Units of coordinate increment and value | Constant |
| CUNIT2A | S*3 | Deg | Units of coordinate increment and value | Constant |
| DATAAVG | R*4 | Any | Average pixel value of non-zero pixels | Derived |
| DATAMAX | R*4 | Any | Maximum value of the image (< DSATVAL). | Derived |
| DATAMDN | R*4 | Any | Median pixel value of non-zero pixels | Derived |
| DATAMIN | R*4 | Any | Minimum value of the image. | Derived |
| DATAP01 | R*4 | Any | Value at 1% of histogram | Derived |
| DATAP10 | R*4 | Any | Value at 10% of histogram | Derived |

| KEYWORD | TYPE | VALUES | DESCRIPTION | SOURCE |
|---|---|---|---|---|
| DATAP25 | R*4 | Any | Value at 25% of histogram | Derived |
| DATAP50 | R*4 | Any | Value at 50% of histogram | Derived |
| DATAP75 | R*4 | Any | Value at 75% of histogram | Derived |
| DATAP90 | R*4 | Any | Value at 90% of histogram | Derived |
| DATAP95 | R*4 | Any | Value at 95% of histogram | Derived |
| DATAP98 | R*4 | Any | Value at 98% of histogram | Derived |
| DATAP99 | R*4 | Any | Value at 99% of histogram | Derived |
| DATASAT | I*4 | Any | Number of pixels saturated | Derived |
| DATASIG | R*4 | Any | Standard deviation of pixel values of non-zero pixels | Derived |
| DATASUM | S | | unsigned integer value of the 32-bit 1's complement checksum of the data | Pipeline |
| DATAZER | I*4 | Any | Number of pixels = 0 | Derived |
| DATE | S*23 | Any | <YYYY-MM-DDThh:mm:ss[.sss]> [UTC] time of FITS file creation | Pipeline |
| DATE_AVG | S*23 | Any | <YYYY-MM-DDThh:mm:ss[.sss]> [UTC] midpoint of observation | Derived |
| DATE_BEG | S*23 | Any | <YYYY-MM-DDThh:mm:ss[.sss]> [UTC] start time of exposure for observation | FSW basehdr.actexptimecoarse, basehdr.actexptimefine |
| DATE_EAR | S*23 | Any | <YYYY-MM-DDThh:mm:ss[.sss]> Start time of observation, corrected to Earth | Derived |
| DATE_END | S*23 | Any | <YYYY-MM-DDThh:mm:ss[.sss]> [UTC] end of readout of last image of the observation | TELAPSE |

| KEYWORD | TYPE | VALUES | DESCRIPTION | SOURCE |
|---|---|---|---|---|
| DATE_OBS | S*23 | Any | DATE_BEG | FSW basehdr.actexptimecoarse, basehdr.actexptimefine |
| DATE_SUN | S*23 | Any | <YYYY-MM-DDThh:mm:ss[.sss]> Start time of observation, corrected to Sun | Derived |
| DETECT_T | R*4 | Any | Detector Temperature | Instrument HK |
| DETECTOR | I*2 | 1-4 | Detector tile number | BSF basehdr.detector |
| DOORPOS | I*1 | 0,1,2 | Telescope door state (0=Closed, 1=In Transit, 2=Open) | FSW basehdr.actualdoorposition |
| DRB_T | R*4 | Any | DRB Temperature | Instrument HK |
| DSATVAL | I*4 | Any | Value used as saturated | Derived |
| DSTART1 | I*2 | 1 | First column of image area on data array | Pipeline |
| DSTART2 | I*2 | 1 | First row of image area | Pipeline |
| DSTOP1 | I*2 | Any | Last column of image area | Pipeline |
| DSTOP2 | I*2 | Any | Last row of image area | Pipeline |
| DSUN_OBS | R*8 | m | S/C distance from Sun | Sunspice |
| EAR_TDEL | R*8 | sec | Time(Sun to Earth) - Time(Sun to S/C) | Sunspice |
| EXTEND | L | T(F) | Indicates that there is (not) an extension | Pipeline |
| FILE_RAW | S*12 | Any | Downloaded image filename | FSW basehdr.filename |

| KEYWORD | TYPE | VALUES | DESCRIPTION | SOURCE |
|---|---|---|---|---|
| FILENAME | S*42 | --> | Name of the FITS file: solo_<level>_<descriptor>_<datetime>_Vxx.fits; descriptor contains information on tile and image specification (see Section 4 for details); datetime is from MET and fixed epoch, Example: solo_L1_solohi-1ff_20201012T045612_V00.fits | Derived |
| FINAL | L | F(T) | T if Released version, F if quicklook | Pipeline |
| GAINCMD | S*2 | AB | Commanded Gain values used in camera where A=PGA_LEV1 and B=PGA_LEV0 | BSF basehdr.gain |
| GAINMODE | S*6 | LOW, HIGH, SIMADC | Gain mode of microcode used, or simulated image | Derived from basehdr.gainmode and shdr.ccucode |
| GSEX_OBS | R*8 | m | S/C Geocentric Solar Ecliptic X | Sunspice |
| GSEY_OBS | R*8 | m | S/C Geocentric Solar Ecliptic Y | Sunspice |
| GSEZ_OBS | R*8 | m | S/C Geocentric Solar Ecliptic Z | Sunspice |
| HAEX_OBS | R*8 | m | S/C Heliocentric Aries Ecliptic X P | Sunspice |
| HAEY_OBS | R*8 | m | S/C Heliocentric Aries Ecliptic Y P | Sunspice |
| HAEZ_OBS | R*8 | m | S/C Heliocentric Aries Ecliptic Z P | Sunspice |
| HCIX_OBS | R*8 | m | S/C Heliocentric Inertial X P | Sunspice |
| HCIX_VOB | R*8 | m/s | S/C Heliocentric Inertial X Velocity P | Sunspice |
| HCIY_OBS | R*8 | m | S/C Heliocentric Inertial Y P | Sunspice |
| HCIY_VOB | R*8 | m/s | S/C Heliocentric Inertial Y Velocity | Sunspice |
| HCIZ_OBS | R*8 | m/s | S/C Heliocentric Inertial Z P | Sunspice |

| KEYWORD | TYPE | VALUES | DESCRIPTION | SOURCE |
|---|---|---|---|---|
| HCIZ_VOB | R*8 | m/s | S/C Heliocentric Inertial Z Velocity | Sunspice |
| HEEX_OBS | R*8 | m | S/C Heliocentric Earth Ecliptic X | Sunspice |
| HEEY_OBS | R*8 | m | S/C Heliocentric Earth Ecliptic Y | Sunspice |
| HEEZ_OBS | R*8 | m | S/C Heliocentric Earth Ecliptic Z | Sunspice |
| HEQX_OBS | R*8 | m | S/C Heliocentric Earth Equatorial P | Sunspice |
| HEQY_OBS | R*8 | m | S/C Heliocentric Earth Equatorial P | Sunspice |
| HEQZ_OBS | R*8 | m | S/C Heliocentric Earth Equatorial Z | Sunspice |
| HGLN_OBS | R*8 | Deg | S/C heliographic longitude | Sunspice |
| HGLT_OBS | R*8 | Deg | S/C heliographic latitude | Sunspice |
| HISTORY | S*71 | Any | Comments of processing history. Can be repeated. | Varies |
| IMGCTR | I*2 | Any | Overall image counter | FSW basehdr.imgCtr |
| IMGSEQ | I*2 | Any | Image sequence counter e.g. nth in sequence | FSW basehdr.imgseq |
| IMGTYPE | S | | enum eImageTypeCodes { OP_NORMAL = 0 // readout, OP_32NORM = 1 // 32 bit readout , OP_32HIGH = 2 // 32 bit high byte, OP_32LOW = 3 // 32 bit low byte , OP_ISTAKE = 4 // Diagnostic , OP_IPTEST = 5 // Diagnostic (IPTESTBUFFER) (ISTAKEIMAGE) , OP_LOWLAT = 6 // Low latency 16 bit pix , NOP_INIT = 7 //NOP INIT , NOP_BEGIN = 8 //NOP Begin , NOP_EOF = 9 , NOP_CMD1 = 17 //NOP Read Script , NOP_NONE = 18 , OP_DEFAULT = 19} | FSW basehdr.imageType |
| INSTRUME | S*6 | SoloHI | Instrument name | Definition |

| KEYWORD | TYPE | VALUES | DESCRIPTION | SOURCE |
|---|---|---|---|---|
| IP_00_19 | S*60 | numeral chars | Function codes of values 0 - 19 in ipCmd (commanded); ref ipcodes.h | FSW basehdr.ipCmd |
| IP_FUNC | I*2 | Any | Row from image processing table used | BSF basehdr.ipfunction |
| IP_PROG | S*? | Any | String representation of ipCmdLog (actual) | FSW basehdr.ipCmdLog |
| IP_TIMEH | R | Any | MET at start of IP (from header) | FSW basehdr.ipprocessingtime |
| IP_TIMET | I*2 | Any | Duration, start of IP to end of IP (from trailer) | Derived from trailer.ipprocessingtime |
| IPCMDCNT | I*2 | | Number of IP functions executed | FSW basehdr.ipCmdCnt |
| IPTRUNC | I*2 | Any | Truncation exponent (data is divided by 2^IPTRUNC) | FSW basehdr.ccLastSUM |
| LATPOLE | R*8 | Deg | Native longitude of the celestial pole | Constant |
| LATPOLEA | R*8 | Deg | Native longitude of the celestial pole | Constant |
| LED1 | I*2 | | Commanded setting of LED1 | BSF basehdr.cmdled1 |
| LED2 | I*2 | | Commanded setting of LED2 | BSF basehdr.cmdled2 |
| LENS_T | R*4 | Any | Lens Temperature | Instrument HK |
| LEVEL | S*3 | CAL, L1, L1b | Data processing level | Pipeline |
| LONPOLE | R*8 | Deg | Native longitude of the celestial pole | Constant |
| LONPOLEA | R*8 | Deg | Native longitude of the celestial pole | Constant |
| NAXIS | I*2 | 0,2,3 | Number of axes in the image (0 indicates header only) | FITS |

| KEYWORD | TYPE | VALUES | DESCRIPTION | SOURCE |
|---|---|---|---|---|
| NAXIS1 | I*2 | Positive | Length of the first axis (columns,x) | FITS |
| NAXIS2 | I*2 | Positive | Length of the second axis (rows,y) | FITS |
| NBIN | R*4 | n^2 | Number of pixels binned; this will change to reflect any correction to the data. = NBIN1 * NBIN2 | Derived |
| NBIN1 | R*4 | n^2 | Number of pixels binned along axis1; this will change to reflect changes in dimension. | FSW basehdr.SUMCOL, basehdr.SEBXSUM |
| NBIN2 | R*4 | n^2 | Number of pixels binned along axis2; this will change to reflect changes in dimension. | FSW basehdr.SUMROW, basehdr.SEBYSUM |
| NSUMEXP | I*2 | Any | Number of exposures added together | BSF basehdr.numsum |
| NUMINSEQ | I*2 | Any | Number of readouts in 1 cycle - from ucode | FSW basehdr.numinseq |
| OBJECT | S | LLDP, more TBD | Full Frame, Subfield (TBD) | Pipeline |
| OBS_ID | S | Any | Unique ID of the individual observation | JSON file |
| OBS_MODE | S | LED, more TBD | Description of the observation mode or 'study' that has been used to acquire this image | JSON file |
| OBS_TYPE | S | Any | Encoded version of obsmode | JSON file |
| OBS_VR | R*8 | Any | [m/s] Radial velocity of spacecraft relative to Sun | Sunspice |
| OBSRVTRY | S*18 | Solar Orbiter | Satellite name | Definition |
| OBT_BEG | R*8 | Any | MET start first exposure | FSW basehdr.actexptimecoarse, basehdr.actexptimefine |

| KEYWORD | TYPE | VALUES | DESCRIPTION | SOURCE |
|---|---|---|---|---|
| OBT_END | R | Any | MET end last exposure | Derived from TELAPSE |
| OFFSET | I*2 | Any | Commanded offset value used in camera | BSF basehdr.offset |
| ORIGIN | S*3 | NRL | SSOC, Solar Orbiter Science Operations Centre | Pipeline |
| PARENT | S | Any | XML packet filename, or name of previous level file | Pipeline |
| PC1_1 | R*8 | Rad | Coordinate transformation matrix element (roll) | Sunspice |
| PC1_1A | R*8 | Rad | Coordinate transformation matrix element (roll) | Sunspice |
| PC1_2 | R*8 | Rad | Coordinate transformation matrix element (roll) | Sunspice |
| PC1_2A | R*8 | Rad | Coordinate transformation matrix element (roll) | Sunspice |
| PC2_1 | R*8 | Rad | Coordinate transformation matrix element (roll) | Sunspice |
| PC2_1A | R*8 | Rad | Coordinate transformation matrix element (roll) | Sunspice |
| PC2_2 | R*8 | Rad | Coordinate transformation matrix element (roll) | Sunspice |
| PC2_2A | R*8 | Rad | Coordinate transformation matrix element (roll) | Sunspice |
| PV1_1 | R*8 | Deg | Native longitude of the reference point | Constant |
| PV1_1A | R*8 | Deg | Native longitude of the reference point | Constant |

| KEYWORD | TYPE | VALUES | DESCRIPTION | SOURCE |
|---|---|---|---|---|
| PV1_2 | R*8 | Deg | Native latitude of the reference point | Constant |
| PV1_2A | R*8 | Deg | Native latitude of the reference point | Constant |
| PV1_3 | R*8 | Deg | Alias for LONPOLE (has precedence) | Constant |
| PV1_3A | R*8 | Deg | Alias for LONPOLE (has precedence) | Constant |
| PV2_0 | R*8 | Any | ZPN projection parameter | Constant |
| PV2_0A | R*8 | Any | ZPN projection parameter | Constant |
| PV2_1 | R*8 | Any | ZPN projection parameter | Constant |
| PV2_1A | R*8 | Any | ZPN projection parameter | Constant |
| PV2_2 | R*8 | Any | ZPN projection parameter | Constant |
| PV2_2A | R*8 | Any | ZPN projection parameter | Constant |
| PV2_3 | R*8 | Any | ZPN projection parameter | Constant |
| PV2_3A | R*8 | Any | ZPN projection parameter | Constant |
| PV2_4 | R*8 | Any | ZPN projection parameter | Constant |
| PV2_4A | R*8 | Any | ZPN projection parameter | Constant |
| PV2_5 | R*8 | Any | ZPN projection parameter | Constant |
| PV2_5A | R*8 | Any | ZPN projection parameter | Constant |
| PXBEG1 | R*4 | Any | First read-out detector column in unrectified detector coordinates | BSF basehdr.p1col |

| KEYWORD | TYPE | VALUES | DESCRIPTION | SOURCE |
|---|---|---|---|---|
| PXBEG2 | R*6 | Any | First read-out detector row in unrectified detector coordinates | BSF basehdr.p1row |
| PXEND1 | R*5 | Any | Last read-out detector column in unrectified detector coordinates | BSF basehdr.p2col |
| PXEND2 | R*7 | Any | Last read-out detector row | BSF basehdr.p2row |
| R1COL | I*2 | 1-2048 | Rectified position of 1st column of image on detector (starting at 1) | Derived |
| R1ROW | I*2 | 1-2048 | rectified Position of 1st row of image on detector | Derived |
| R2COL | I*2 | 1-2048 | rectified Position of last column of image on detector | Derived |
| R2ROW | I*2 | 1-2048 | rectified Position of last row of image on detector | Derived |
| READTIME | I*16 | Any | Time to readout raw image from camera in usec | Derived |
| RECTIFY | L | F(T) | Put ecliptic north to the top of the image | Pipeline |
| RECTROTA | I*1 | 0-7 | Argument for rotate.pro to put ecliptic north at top of image | Pipeline |
| REGION | I*1 | 1-4 | Subfield region of tile based on number of regions from a given tile in a specific sequence | BSF basehdr.region |
| RSUN_ARC | R*8 | Arcesec | Photospheric solar radius | Sunspice |
| RSUN_REF | R*8 | m | Assumed physical solar radius | Sunspice |
| SA_ROTYP | R*4 | Any | Solar array rotation angle +Y | S/C HK |

| KEYWORD | TYPE | VALUES | DESCRIPTION | SOURCE |
|---|---|---|---|---|
| SA_ROTYM | R*4 | Any | Solar array rotation angle -Y | S/C HK |
| SC_PITCH | R*4 | Deg | S/C pitch at DATE-AVG | Sunspice |
| SC_ROLL | R*4 | Deg | S/C roll at DATE-AVG | Sunspice |
| SC_YAW | R*4 | Deg | S/C yaw at DATE-AVG | Sunspice |
| SEBXSUM | I*2 | Any | 18 Number columns being summed in IP | FSW basehdr.sebxsum |
| SEBYSUM | I*2 | Any | 19 Number rows being summed in IP | FSW basehdr.sebysum |
| SEQUCODE | S*3 | Any | Subscript of Sequencer Microcode from ucdtbldt.img or isreadout.cpp for this image (5 LSB of ccIsUcode) | FSW basehdr.ccisucode |
| SIMPLE | L | T | Conforms to FITS standard | FITS |
| SOLAR_EP | R*8 | Deg | S/C ecliptic North to solar North angle | Sunspice |
| SOOPNAME | S*23 | Any | Name of the SOOP Campaign that the data belong to | JSON file |
| SOOPTYPE | S | Any | Encoded identification of the<br><br>SOOP(s) that this observation belongs to. | JSON file |
| SUMCOL | | uint16, | Number colums being summed in CC | BSF basehdr.sumrow |
| SUMROW | | uint16, | Number rows being summed in CC | BSF basehdr.sumrow |
| SUN_TIME | R*8 | Sec | Time(Sun to S/C) | Sunspice |
| TARGET | S | Any | 'AR' Type of target from planning (TBD) | Pipeline |
| TELAPSE | R | Sec | Elapsed time between beginning and end of observation | FSW basehdr.totalexpduration |

| KEYWORD | TYPE | VALUES | DESCRIPTION | SOURCE |
|---|---|---|---|---|
| TELESCOP | S | SOLO/SoloHI/[1234] | ID of data source | Pipeline |
| TIMESYS | S*3 | UTC | system used for time keywords | Pipeline |
| TIMGCTR | I*2 | Any | Counter from load ucode for each ROI(?) | FSW basehdr.telescopeImgCnt |
| VERS_CAL | S*8 | HHSSS | L1/CAL: hex representation of HH: header version, SSS: make_solohi_hdr.pro version. | Pipeline |
| VERS_SW | S*8 | Any | CVS version of solohi_reduce.pro | Pipeline |
| VERSION | S*2 | 01,02… | FITS File version number (same as filename if Released) or date and time for LL | Pipeline |
| WAVEBAND | S | VISIBLE | ID of the spectral line list | Constant |
| WAVELNTH | R*4 | 5400.0 | Bandpass peak response (Angstroms) | Calibration |
| WCSAXES | I*2 | 2 | Number of coordinate axes | Definition |
| WCSNAME | S*25 | Helioprojective Zenith Polynomial', | Coordinate System | Definition |
| XFBYTES | I*4 | Any | Number of bytes sent | Pipeline derived |
| XPOSURE | R*4 | Sec | Effective exposure time | Pipeline derived |